Dynamical Correlations and Screened Exchange on the Experimental Bench: Spectral Properties of the Cobalt Pnictide $BaCo_2As_2$

Ambroise van Roekeghem,[1,2,*] Thomas Ayral,[2,3] Jan M. Tomczak,[4] Michele Casula,[5] Nan Xu,[1,6] Hong Ding,[1,7] Michel Ferrero,[2] Olivier Parcollet,[3] Hong Jiang,[8] and Silke Biermann[2,9]

[1]*Beijing National Laboratory for Condensed Matter Physics, and Institute of Physics, Chinese Academy of Sciences, Beijing 100190, China*

[2]*Centre de Physique Théorique, Ecole Polytechnique, CNRS UMR 7644, 91128 Palaiseau, France*

[3]*Institut de Physique Théorique (IPhT), CEA, CNRS, URA 2306, 91191 Gif-sur-Yvette, France*

[4]*Institute of Solid State Physics, Vienna University of Technology, A-1040 Vienna, Austria*

[5]*CNRS and Institut de Minéralogie, de Physique des Matériaux et de Cosmochimie, Université Pierre et Marie Curie, case 115, 4 place Jussieu, FR-75252 Paris Cedex 05, France*

[6]*Swiss Light Source, Paul Scherrer Institut, CH-5232 Villigen, Switzerland*

[7]*Collaborative Innovation Center of Quantum Matter, Beijing 100190, China*

[8]*College of Chemistry and Molecular Engineering, Peking University, 100871 Beijing, China*

[9]*Collège de France, 11 place Marcelin Berthelot, 75005 Paris, France*

(Received 13 August 2014; published 24 December 2014)

Understanding the Fermi surface and low-energy excitations of iron or cobalt pnictides is crucial for assessing electronic instabilities such as magnetic or superconducting states. Here, we propose and implement a new approach to compute the low-energy properties of correlated electron materials, taking into account both screened exchange beyond the local density approximation and local dynamical correlations. The scheme allows us to resolve the puzzle of $BaCo_2As_2$, for which standard electronic structure techniques predict a ferromagnetic instability not observed in nature.

DOI: 10.1103/PhysRevLett.113.266403 PACS numbers: 71.27.+a, 71.10.-w, 71.45.Gm, 74.70.Xa

The discovery of unconventional superconductivity in iron pnictides in 2008 has aroused strong interest in the Fermi surfaces and low-energy excitations of transition metal pnictides. Angle-resolved photoemission spectroscopy (ARPES) has been used to systematically map out quasiparticle dispersions, and to identify electron and hole pockets potentially relevant for low-energy instabilities [1–7]. Density functional theory (DFT) calculations have complemented the picture, yielding information about orbital characters [8], or the dependence of the topology of the Fermi surface on structural parameters or element substitution [9,10]. DFT within the local density approximation (LDA) or generalized gradient schemes has also served as a starting point for refined many-body calculations (see, e.g., Refs. [11–18]). Its combination with dynamical mean field theory (LDA + DMFT) [19–25] is nowadays the state-of-the-art *ab initio* many-body approach to low-energy properties of transition metal pnictides. Despite tremendous successes, however, limitations have also been pointed out, e.g., in the description of the Fermi surfaces. Prominent examples include $Ba(Fe,Co)_2As_2$ [26,27] or LiFeAs [14,26]. Interestingly, many-body perturbation theory approximating the self-energy by its first order term in the screened Coulomb interaction W (so-called "GW approximation") results in a substantially improved description: calculations using the quasiparticle self-consistent (QS) GW method [28] have pinpointed nonlocal self-energy corrections to the LDA Fermi surfaces not captured in LDA + DMFT as pivotal [26]. Yet, as a perturbative method, the GW approximation cannot describe materials away from the weak coupling limit [29], and the description of incoherent regimes [13,17] including coherence-incoherence crossovers [30], local moment behavior [15], or the subtle effects of doping or temperature changes [17] are still reserved for DMFT.

In this Letter, we propose and implement a new approach to the spectral properties of correlated electron materials taking into account screened exchange beyond the LDA and correlations as described by DMFT with frequency-dependent local Hubbard interactions. The approach can be understood as a simplified and extremely efficient version of the combined GW + DMFT method [31], as a nonperturbative dynamical generalization of the popular "Coulomb-hole-screened-exchange" ("COHSEX") scheme [32], or as a combination of generalized Kohn-Sham schemes [33,34] with DMFT. We demonstrate the validity of our combined "screened exchange+dynamical DMFT" (SEx+DDMFT) scheme by calculating the spectral function of $BaCo_2As_2$ for which detailed ARPES results are available [35,36]. Finally, our work sheds new light on the physical justifications of electronic structure techniques that combine DFT with DMFT, by revealing a subtle error cancellation between nonlocal exchange and dynamical screening effects, both neglected in standard methods.

Our target compound $BaCo_2As_2$ is isostructural to the prototypical compound of the so-called 122 iron-based superconductors, $BaFe_2As_2$. Replacing Fe by Co, however,

increases the filling to a nominal $3d^7$ configuration, with drastic consequences: whereas compounds with filling around the d^6 configuration exhibit characteristic power law deviations from Fermi liquid behavior above often extremely low coherence temperatures [17], in $BaCo_2As_2$ ARPES identifies clearly defined long-lived quasiparticle bands with relatively weak mass renormalizations [35]. Nevertheless, the electronic structure of this compound raises puzzling questions concerning its paramagnetic behavior: DFT calculations predict a huge density of states (DOS) at the Fermi level, which, given the large Stoner parameter of Co, would be expected to trigger a ferromagnetic instability [37]. The DOS of the isoelectronic compound $SrCo_2As_2$ presents the same features, but the maximum lies just below the Fermi level [38]. Still, in $SrCo_2As_2$—also a paramagnet—important antiferromagnetic fluctuations have been measured, possibly competing with ferromagnetic order [38,39]. $CaCo_2As_2$, $Ca_{0.9}Sr_{0.1}Co_2As_2$, and $CaCo_{1.86}As_2$ exhibit magnetic phases with in-plane ferromagnetism at low temperatures [40–42]. ARPES data of $BaCo_2As_2$ show that there is indeed a flat band (dominantly of $d_{x^2-y^2}$ character) close to the Fermi surface, albeit less filled than predicted by LDA calculations [35,36], suggesting $BaCo_2As_2$ to be on the verge of a transition [43]. This compound is thus an ideal benchmark system, on which to test new theoretical approaches.

We start our analysis by comparing results for the spectral function calculated within standard LDA + DMFT and LDA + DMFT with frequency-dependent local Hubbard interactions $\mathcal{U}(\omega)$ to the ARPES spectral function of Ref. [35] (Fig. 1). The latter scheme will be abbreviated in the following as LDA + DDMFT to stress the doubly dynamical nature of the theory, which determines a frequency-dependent self-energy in the DMFT spirit, extended, however, to frequency-dependent interactions [17,44,45]. The effective local interactions used in the DMFT calculations were obtained within the constrained random phase approximation in the implementation of Ref. [53]. For LDA + DDMFT, the full frequency-dependence of the monopole term $F_0(\omega)$ is retained in the calculation. The effective local problem with dynamical $\mathcal{U}$ is solved self-consistently by means of a continuous-time Monte Carlo algorithm [54,55] that we have implemented within the TRIQS toolbox [56].

Electronic bands in the energy window between the Fermi level and −2 eV binding energy are states of predominant Co-3d character, and undergo—even in this quite moderately correlated compound—a non-negligible band renormalization, as compared to the LDA band structure [Fig. 1(a)]. Standard LDA + DMFT [Fig. 1(b)] captures this effect, leading to a reduced bandwidth in good agreement with the ARPES results. When dynamical screening effects are taken into account [Fig. 1(c)], additional renormalizations occur, corresponding to the electronic polaron effect discussed in Ref. [57], and the overall

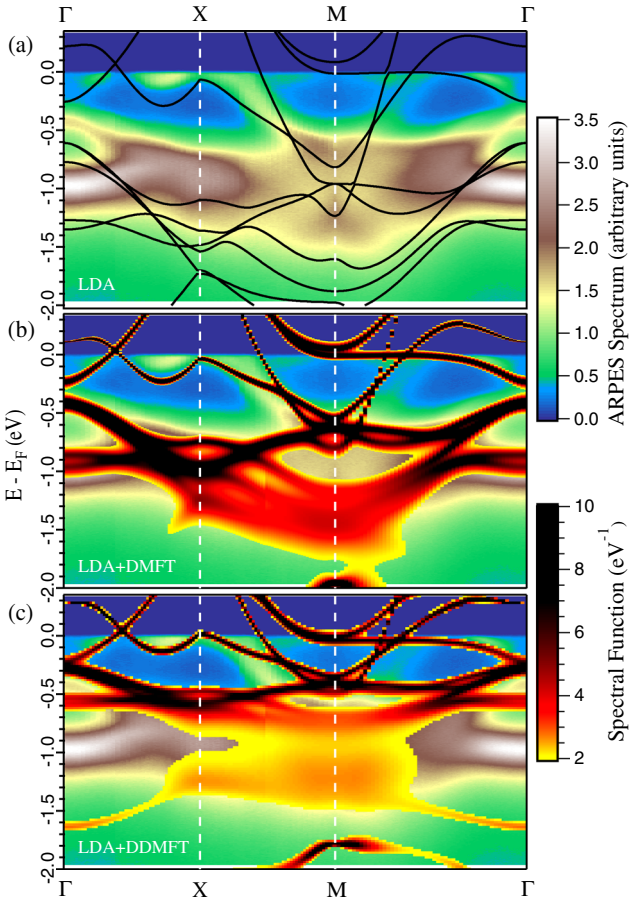

FIG. 1 (color online). $BaCo_2As_2$ photoemission spectra, replotted from Ref. [35]. Superimposed are (a) the Kohn-Sham band structure of the DFT LDA, (b) the spectral function of standard LDA + DMFT [only those parts that exceed 2 states/eV are shown], (c) the spectral function within LDA + DDMFT [same representation as in (b)].

bandwidth reduction appears to be overestimated. However, one should not conclude from this analysis that dynamical screening effects are absent. Rather, nonlocal exchange—routinely neglected in DFT-based techniques—reshapes and widens the quasiparticle band structure, and the apparent success of LDA + DMFT in obtaining the correct quasiparticle bandwidth relies on an error cancellation when both dynamical screening and nonlocal exchange are neglected in the calculation of the spectral function. We will now substantiate this claim by explicitly including screened exchange, and performing a DMFT calculation with dynamical Hubbard interactions based on the following one-particle Hamiltonian: $H_0 = H_{\mathrm{Hartree}} + H_{\mathrm{SEx}}$, where the first term denotes the Hamiltonian of the system at the Hartree mean-field level, evaluated at the self-consistent DFT-LDA density. H_{SEx} is a screened Fock exchange term, calculated from the Yukawa potential $e^2\exp(-k_{\mathrm{TF}}|r-r'|)/|r-r'|$ with screening wavevector k_{TF}. This scheme can be understood as the next generation after the recent LDA + DDMFT scheme, by replacing the

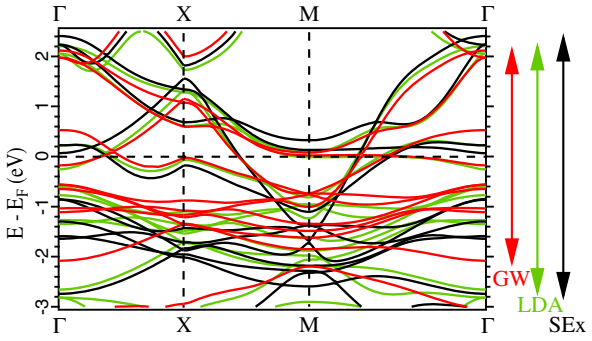

FIG. 2 (color online). Comparison of band structures of $BaCo_2As_2$ in the $k_z = 0$ plane calculated within the QS GW (red), LDA (green), and screened-exchange (black) schemes.

local Kohn-Sham exchange-correlation potential of DFT by a nonlocal screened Fock exchange term [58].

We first analyze the band structure corresponding to H_0 alone, in comparison to the LDA band structure and the one obtained from the QSGW method (in the implementation of Ref. [61]), see Fig. 2. As expected, the inclusion of nonlocal exchange in H_0 increases the delocalization of electrons, and thus widens the bands as compared to the LDA electronic structure. In the QSGW method, this effect is overcompensated by correlation-induced band narrowing, and the bandwidth of $3d$-like bands is about 15% smaller than in the LDA. These comparisons highlight the fact that—taking the screened exchange band structure as a reference—the effective exchange-correlation potential of DFT not only incorporates exchange (in a local fashion), but also mimics band renormalizations due to correlations (yet without keeping track of the corresponding spectral weight transfers).

We finally turn to the results of our new scheme: Fig. 3 displays the spectral function within SEx + DDMFT [panel (a)], superimposed on the ARPES data [panel (b)]. The overall spectrum from SEx + DDMFT is very close to the experiment: the bandwidth, Fermi surface, and band renormalizations close to the Fermi level are correctly predicted.

The orbital-resolved electron count obtained with SEx + DDMFT is displayed in Table I and compared to the one within the other schemes. The orbital polarization from the LDA is reduced by correlations, and nearly suppressed within LDA + DDMFT. Conversely, screened exchange increases the orbital polarization, and the final SEx + DDMFT result still displays stronger orbital polarization than the LDA. This trend can be related to the weakly dispersive $d_{x^2-y^2}$ states discussed above: as in the SEx band dispersion of Fig. 2, the effect of screened exchange is to push the flat $d_{x^2-y^2}$-like band away from the Fermi level, to the point of suppressing the electron pocket at the Γ point. This does not correspond to the experimental spectrum, and indeed it is corrected by including correlations. Figure 4 displays the low-energy spectra along the ΓM direction

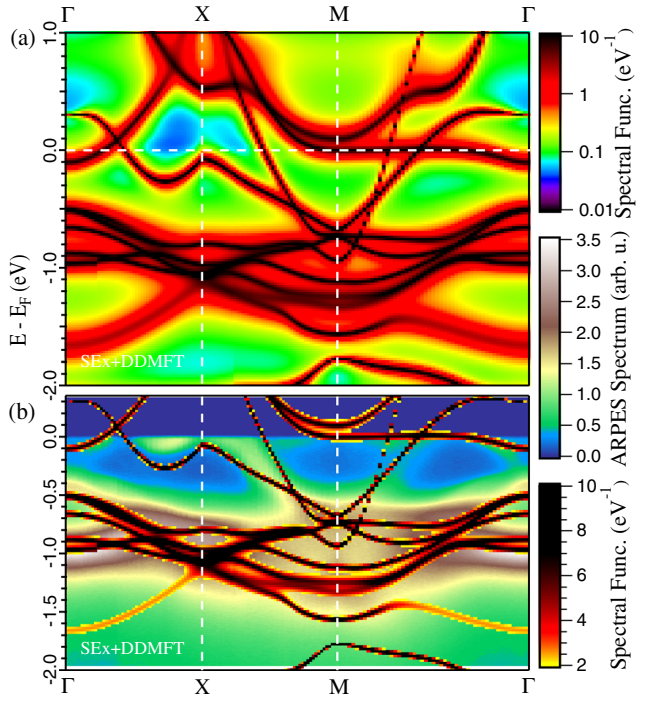

FIG. 3 (color online). $BaCo_2As_2$ within screened exchange + DDMFT: (a) spectral function and (b) bands extracted from the maxima of panel (a) and superimposed on ARPES data as in Fig. 1.

comparing SEx + DDMFT and LDA + DMFT overlaid onto the second derivative of the ARPES data [62], together with the QSGW band dispersion. The electron pocket at Γ is recovered in SEx + DDMFT, and the fraction of $d_{x^2-y^2}$ electrons increases. Within the LDA, the flat band is nearly filled along the ΓM direction, and even more so when we take into account correlations. According to ARPES, this flat band should be occupied only in a small electron pocket at Γ, containing about 0.18 e^-. This result is consistent with the absence of ferromagnetism. Indeed, this flat band lying on the Fermi surface would imply a high density of states at the Fermi level that could trigger a Stoner instability. We extract from the SEx + DDMFT calculations a DOS at the Fermi energy of 0.97 states/eV/Co/spin. Assuming a Stoner parameter of ∼0.9 eV, this leaves us slightly below the onset of Stoner ferromagnetism [63].

TABLE I. Number of electrons in cobalt-d Wannier functions within the LDA, SEx, SEx+DDMFT, LDA + DMFT, and LDA + DDMFT schemes.

	n^e_{LDA}	n^e_{SEx}	$n^e_{\mathrm{SEx+DDMFT}}$	$n^e_{\mathrm{LDA+DMFT}}$	$n^e_{\mathrm{LDA+DDMFT}}$
d_{z^2}	1.64	1.66	1.63	1.61	1.62
$d_{x^2-y^2}$	1.49	1.27	1.37	1.53	1.59
d_{xy}	1.74	1.78	1.72	1.67	1.63
d_{xz}/d_{yz}	1.69	1.73	1.68	1.64	1.62
Total	8.24	8.16	8.08	8.09	8.09

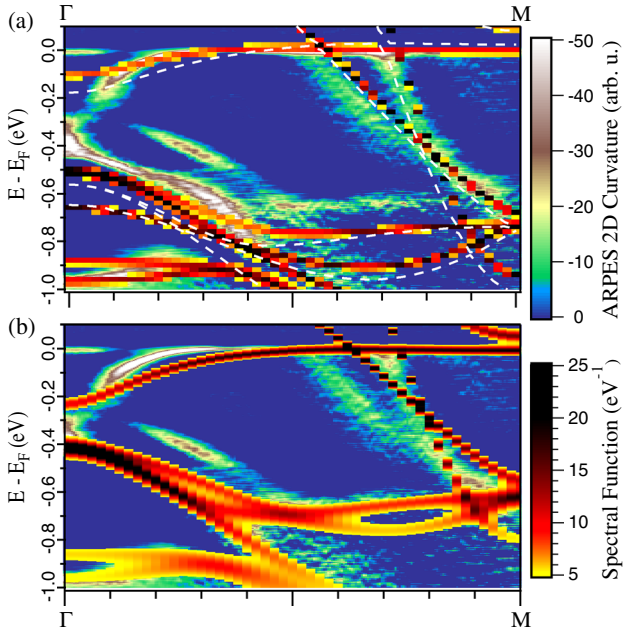

FIG. 4 (color online). Bands along the Γ*M* direction, extracted from the spectral function calculated by (a) SEx + DDMFT and (b) LDA + DMFT, superimposed on ARPES data from Ref. [35] (represented as a second derivative of the photoemission intensity). The QS*GW* band structure is also given (white dashed lines).

The QS*GW* scheme also provides an overall good description, including the position of the $d_{x^2-y^2}$ band, its filling, and its related Fermi wave vector. Taking nonlocal exchange into account is thus necessary to capture the physics of $BaCo_2As_2$, and our SEx + DDMFT scheme performs well for these subtle effects.

Finally, we put our new computational scheme in perspective. As far as coarse features such as the bandwidth are concerned, standard LDA + DMFT and the new SEx + DDMFT give comparable results, providing an *a posteriori* explanation for the success of LDA + DMFT calculations with static interactions. For total energy calculations within DFT, it is well known that there are subtle error cancellations between the exchange and correlation contributions in approximate density functionals. Here, we evidence a similar behavior for spectral properties. The effect of dynamical screening as incorporated in the high-energy tail of the dynamical Hubbard interaction $\mathcal{U}(\omega)$ can roughly be understood as a band narrowing by a factor $Z_B = \exp[-\int_0^\infty d\omega \Im\mathcal{U}(\omega)/(\pi\omega^2)]$ [64]. For $BaCo_2As_2$, we find dynamical screening to be non-negligible, with $Z_B \sim 0.6$. LDA + DDMFT double counts this narrowing effect, as the bandwidth has already been decreased by correlations hidden in the exchange-correlation functional, with respect to the Hartree-Fock or SEx band structure. Thus, starting a many-body calculation from the LDA raises not only the usual well-known double counting questions related to the energetic position of correlated versus itinerant states, but even more serious ones related to the double counting of screening processes. SEx + DDMFT avoids these issues, providing a more solid foundation for the investigation of dynamical screening effects. On a more pragmatic level, the similarity of the LDA + DMFT and SEx + DDMFT spectral functions suggests that error cancellations between dynamical screening and nonlocal exchange, both absent in LDA + DMFT, make this scheme suitable at least for questions concerning the overall bandwidth reduction of correlated electron systems. Finer details related to the very low energy behavior or Fermi surface topologies, on the other hand, might require explicit exchange corrections as introduced in the present work.

In summary, we have shown that screened exchange combined with dynamical correlations provides an excellent description of the low-energy physics in $BaCo_2As_2$. In contrast to perturbative schemes, it can be expected that our nonperturbative method can be extended to regimes with arbitrarily strong correlations, making it a promising tool for probing the finite temperature normal state of iron based superconductors. For $BaCo_2As_2$, we show that the flat $d_{x^2-y^2}$ band in the immediate vicinity of the Fermi level is extremely sensitive to an accurate treatment of screened exchange, and that this effect is key to the paramagnetic nature of the compound. Pump-probe photoemission would be useful to experimentally locate the flat band and guide the search for new ways to tune its exact energetic position, thus directly playing on possible Fermi surface instabilities.

We acknowledge useful discussions with V. Brouet, T. Miyake, and the authors of Ref. [35]. This work was supported by the French ANR under project PNICTIDES, IDRIS/GENCI under Projects No. 091393 and No. 96493, the Cai Yuanpei program, and the European Research Council (Projects No. 617196 and No. 278472). J. M. T. acknowledges the hospitality of CPHT within a CNRS visiting position. H. J. acknowledges support by the National Natural Science Foundation of China (Projects No. 20973009 and No. 21173005).

*vanroeke@cpht.polytechnique.fr

[1] H. Ding, P. Richard, K. Nakayama, K. Sugawara, T. Arakane, Y. Sekiba, A. Takayama, S. Souma, T. Sato, T. Takahashi *et al.*, Europhys. Lett. **83**, 47001 (2008).
[2] C. Liu, G. D. Samolyuk, Y. Lee, N. Ni, T. Kondo, A. F. Santander-Syro, S. L. Bud'ko, J. L. McChesney, E. Rotenberg, T. Valla *et al.*, Phys. Rev. Lett. **101**, 177005 (2008).
[3] V. Brouet, M. Marsi, B. Mansart, A. Nicolaou, A. Taleb-Ibrahimi, P. Le Fèvre, F. Bertran, F. Rullier-Albenque, A. Forget, and D. Colson, Phys. Rev. B **80**, 165115 (2009).
[4] T. Shimojima, K. Ishizaka, Y. Ishida, N. Katayama, K. Ohgushi, T. Kiss, M. Okawa, T. Togashi, X.-Y. Wang, C.-T. Chen *et al.*, Phys. Rev. Lett. **104**, 057002 (2010).
[5] S. de Jong, Y. Huang, R. Huisman, F. Massee, S. Thirupathaiah, M. Gorgoi, F. Schaefers, R. Follath,

J. B. Goedkoop, and M. S. Golden, Phys. Rev. B **79**, 115125 (2009).
[6] J. Fink, S. Thirupathaiah, R. Ovsyannikov, H. A. Dürr, R. Follath, Y. Huang, S. de Jong, M. S. Golden, Y.-Z. Zhang, H. O. Jeschke *et al.*, Phys. Rev. B **79**, 155118 (2009).
[7] W. Malaeb, T. Yoshida, A. Fujimori, M. Kubota, K. Ono, K. Kihou, P. M. Shirage, H. Kito, A. Iyo, H. Eisaki *et al.*, J. Phys. Soc. Jpn. **78**, 123706 (2009).
[8] D. J. Singh, Physica (Amsterdam) **469C**, 418 (2009).
[9] V. Vildosola, L. Pourovskii, R. Arita, S. Biermann, and A. Georges, Phys. Rev. B **78**, 064518 (2008).
[10] I. I. Mazin, D. J. Singh, M. D. Johannes, and M. H. Du, Phys. Rev. Lett. **101**, 057003 (2008).
[11] K. Haule, J. H. Shim, and G. Kotliar, Phys. Rev. Lett. **100**, 226402 (2008).
[12] M. Aichhorn, L. Pourovskii, V. Vildosola, M. Ferrero, O. Parcollet, T. Miyake, A. Georges, and S. Biermann, Phys. Rev. B **80**, 085101 (2009).
[13] M. Aichhorn, S. Biermann, T. Miyake, A. Georges, and M. Imada, Phys. Rev. B **82**, 064504 (2010).
[14] J. Ferber, K. Foyevtsova, R. Valentí, and H. O. Jeschke, Phys. Rev. B **85**, 094505 (2012).
[15] P. Hansmann, R. Arita, A. Toschi, S. Sakai, G. Sangiovanni, and K. Held, Phys. Rev. Lett. **104**, 197002 (2010).
[16] V. I. Anisimov, D. Korotin, M. A. Korotin, A. V. Kozhevnikov, J. Kunes, A. O. Shorikov, S. L. Skornyakov, and S. V. Streltsov, J. Phys. Condens. Matter **21**, 075602 (2009).
[17] P. Werner, M. Casula, T. Miyake, F. Aryasetiawan, A. J. Millis, and S. Biermann, Nat. Phys. **8**, 331 (2012).
[18] G. T. Wang, Y. Qian, G. Xu, X. Dai, and Z. Fang, Phys. Rev. Lett. **104**, 047002 (2010).
[19] V. I. Anisimov, A. Poteryaev, M. Korotin, A. Anokhin, and G. Kotliar, J. Phys. Condens. Matter **9**, 7359 (1997).
[20] A. I. Lichtenstein and M. I. Katsnelson, Phys. Rev. B **57**, 6884 (1998).
[21] G. Kotliar and D. Vollhardt, Phys. Today **57**, No. 3, 53 (2004).
[22] S. Biermann, in *Encyclopedia of Materials:Science and Technology*, edited by K. H. J. Buschow, R. W. Cahn, M. C. Flemings, B. Ilschner (print), E. J. Kramer, S. Mahajan, and P. Veyssière (updates) (Elsevier, Oxford, 2006), pp. 1–9.
[23] K. Held, I. A. Nekrasov, G. Keller, V. Eyert, N. Blümer, A. K. McMahan, R. T. Scalettar, T. Pruschke, V. I. Anisimov, and D. Vollhardt, Phys. Status Solidi B **243**, 2599 (2006); psi-k Newsletter, **56** (65) 2003.
[24] G. Kotliar, S. Y. Savrasov, K. Haule, V. S. Oudovenko, O. Parcollet, and C. A. Marianetti, Rev. Mod. Phys. **78**, 865 (2006).
[25] J. Minár, L. Chioncel, A. Perlov, H. Ebert, M. I. Katsnelson, and A. I. Lichtenstein, Phys. Rev. B **72**, 045125 (2005).
[26] J. M. Tomczak, M. van Schilfgaarde, and G. Kotliar, Phys. Rev. Lett. **109**, 237010 (2012).
[27] V. Brouet, P.-H. Lin, Y. Texier, J. Bobroff, A. Taleb-Ibrahimi, P. Le Fèvre, F. Bertran, M. Casula, P. Werner, S. Biermann *et al.*, Phys. Rev. Lett. **110**, 167002 (2013).
[28] M. van Schilfgaarde, T. Kotani, and S. Faleev, Phys. Rev. Lett. **96**, 226402 (2006).
[29] T. Ayral, P. Werner, and S. Biermann, Phys. Rev. Lett. **109**, 226401 (2012).
[30] K. Haule and G. Kotliar, New J. Phys. **11**, 025021 (2009).
[31] S. Biermann, F. Aryasetiawan, and A. Georges, Phys. Rev. Lett. **90**, 086402 (2003).
[32] L. Hedin, Phys. Rev. **139**, A796 (1965).
[33] D. M. Bylander and L. Kleinman, Phys. Rev. B **41**, 7868 (1990).
[34] A. Seidl, A. Görling, P. Vogl, J. A. Majewski, and M. Levy, Phys. Rev. B **53**, 3764 (1996).
[35] N. Xu, P. Richard, A. van Roekeghem, P. Zhang, H. Miao, W.-L. Zhang, T. Qian, M. Ferrero, A. S. Sefat, S. Biermann *et al.*, Phys. Rev. X **3**, 011006 (2013).
[36] R. S. Dhaka, Y. Lee, V. K. Anand, D. C. Johnston, B. N. Harmon, and A. Kaminski, Phys. Rev. B **87**, 214516 (2013).
[37] A. S. Sefat, D. J. Singh, R. Jin, M. A. McGuire, B. C. Sales, and D. Mandrus, Phys. Rev. B **79**, 024512 (2009).
[38] A. Pandey, D. G. Quirinale, W. Jayasekara, A. Sapkota, M. G. Kim, R. S. Dhaka, Y. Lee, T. W. Heitmann, P. W. Stephens, V. Ogloblichev *et al.*, Phys. Rev. B **88**, 014526 (2013).
[39] W. Jayasekara, Y. Lee, A. Pandey, G. S. Tucker, A. Sapkota, J. Lamsal, S. Calder, D. L. Abernathy, J. L. Niedziela, B. N. Harmon *et al.*, Phys. Rev. Lett. **111**, 157001 (2013).
[40] B. Cheng, B. F. Hu, R. H. Yuan, T. Dong, A. F. Fang, Z. G. Chen, G. Xu, Y. G. Shi, P. Zheng, J. L. Luo *et al.*, Phys. Rev. B **85**, 144426 (2012).
[41] J. J. Ying, Y. J. Yan, A. F. Wang, Z. J. Xiang, P. Cheng, G. J. Ye, and X. H. Chen, Phys. Rev. B **85**, 214414 (2012).
[42] V. K. Anand, R. S. Dhaka, Y. Lee, B. N. Harmon, A. Kaminski, and D. C. Johnston, Phys. Rev. B **89**, 214409 (2014).
[43] Indeed, a presentation of the ARPES spectra in a second derivative plot of the intensities reveals the presence of a flat band just above the Fermi level [35], as pointed out in Ref. [36].
[44] M. Casula, A. Rubtsov, and S. Biermann, Phys. Rev. B **85**, 035115 (2012).
[45] See Supplemental Material at http://link.aps.org/supplemental/10.1103/PhysRevLett.113.266403, which includes Refs. [46–52], for technical details.
[46] P. Blaha, K. Schwarz, G. Madsen, D. Kvasnicka, and J. Luitz, *Wien2k, An Augmented Plane Wave+Local Orbitals Program for Calculating Crystal Properties* (Tech. Universität Wien, Austria, 2001).
[47] F. O. Tran and P. Blaha, Phys. Rev. B **83**, 235118 (2011).
[48] L. Vaugier, Ph.D. thesis, Ecole Polytechnique, France, 2011.
[49] V. I. Anisimov, J. Zaanen, and O. K. Andersen, Phys. Rev. B **44**, 943 (1991).
[50] L. Hedin, J. Phys. Condens. Matter **11**, R489 (1999).
[51] K. Morikawa, T. Mizokawa, K. Kobayashi, A. Fujimori, H. Eisaki, S. Uchida, F. Iga, and Y. Nishihara, Phys. Rev. B **52**, 13711 (1995).
[52] A. van Roekeghem and S. Biermann, Europhys. Lett. **108**, 57003 (2014).
[53] L. Vaugier, H. Jiang, and S. Biermann, Phys. Rev. B **86**, 165105 (2012).
[54] P. Werner, A. Comanac, L. de' Medici, M. Troyer, and A. J. Millis, Phys. Rev. Lett. **97**, 076405 (2006).
[55] P. Werner and A. J. Millis, Phys. Rev. Lett. **104**, 146401 (2010).

[56] M. Ferrero and O. Parcollet, TRIQS: A Toolbox for Research on Interacting Quantum Systems, http://ipht.cea.fr/triqs.

[57] M. Casula, P. Werner, L. Vaugier, F. Aryasetiawan, T. Miyake, A. J. Millis, and S. Biermann, Phys. Rev. Lett. **109**, 126408 (2012).

[58] We note that in SEx + DMFT nonlocal and dynamical renormalizations are by construction separated on the self-energy or Hamiltonian level. This separability was recently justified for iron pnictides [26] and found to hold also for metallic transition metal oxides [59,60].

[59] J. M. Tomczak, M. Casula, T. Miyake, and S. Biermann, Phys. Rev. B **90**, 165138 (2014).

[60] J. M. Tomczak, M. Casula, T. Miyake, F. Aryasetiawan, and S. Biermann, Europhys. Lett. **100**, 67001 (2012).

[61] T. Kotani, M. van Schilfgaarde, and S. V. Faleev, Phys. Rev. B **76**, 165106 (2007).

[62] P. Zhang, P. Richard, T. Qian, Y.-M. Xu, X. Dai, and H. Ding, Rev. Sci. Instrum. **82**, 043712 (2011).

[63] However, slight electron doping would bring us close to the maximum value of 1.04 states/eV/Co/spin that we find at $\omega = 44$ meV, at the peak of the Co $d_{x^2-y^2}$ DOS, possibly triggering a ferromagnetic instability.

[64] In the antiadiabatic limit, where the characteristic frequency of variations in $\mathcal{U}(\omega)$ is larger than the other energy scales of the system, this statement can be made rigorous via a Lang-Firsov transformation [57].